


Observation of sizeable ω contribution to $\chi_{c1}(3872) \rightarrow \pi^+ \pi^- J/\psi$ decays

R. Aaij *et al.**
(LHCb Collaboration)

 (Received 26 April 2022; accepted 17 May 2023; published 27 July 2023)

Resonant structures in the dipion mass spectrum from $\chi_{c1}(3872) \rightarrow \pi^+ \pi^- J/\psi$ decays, produced via $B^+ \rightarrow K^+ \chi_{c1}(3872)$ decays, are analyzed using proton-proton collision data collected by the LHCb experiment, corresponding to an integrated luminosity of 9 fb^{-1} . A sizeable contribution from the isospin conserving $\chi_{c1}(3872) \rightarrow \omega J/\psi$ decay is established for the first time, $(21.4 \pm 2.3 \pm 2.0)\%$, with a significance of more than 7.1σ . The amplitude of isospin violating decay, $\chi_{c1}(3872) \rightarrow \rho^0 J/\psi$, relative to isospin conserving decay, $\chi_{c1}(3872) \rightarrow \omega J/\psi$, is properly determined, and it is a factor of 6 larger than expected for a pure charmonium state.

DOI: [10.1103/PhysRevD.108.L011103](https://doi.org/10.1103/PhysRevD.108.L011103)

After the discovery of the $\chi_{c1}(3872)$ state in decays through the $\pi^+ \pi^- J/\psi$ channel [1], the $\rho^0 J/\psi$ process was suggested to explain the observed $\pi^+ \pi^-$ mass ($m_{\pi^+ \pi^-}$) distribution peaking near the upper kinematic limit, close to the ρ^0 pole mass. The isovector nature of the produced $\pi^+ \pi^-$ pairs is also supported by the nonobservation of $\chi_{c1}(3872) \rightarrow \pi^0 \pi^0 J/\psi$ decays. Since no charged partners of the $\chi_{c1}(3872)$ state have been observed in the $\rho^\pm J/\psi$ decay mode [2,3], the $\chi_{c1}(3872)$ particle is predominantly an isosinglet state; the J/ψ isospin is also zero. Together, this makes the $\chi_{c1}(3872) \rightarrow \rho^0 J/\psi$ decay isospin violating. The $\chi_{c1}(3872)$ spin and parities, $J^{PC} = 1^{++}$ [4,5], match the 2^3P_1 excitation of the $c\bar{c}$ system predicted in the relevant mass range [6]. However, isospin violating decays of charmonium states are highly suppressed. Therefore, quantifying the isospin violation in $\chi_{c1}(3872) \rightarrow \rho^0 J/\psi$ decays is important to understand the nature of the $\chi_{c1}(3872)$ state, which is under intense debate [7,8]. Isospin conserving $\chi_{c1}(3872) \rightarrow \omega J/\psi$ decays provide a suitable normalization process. Such decays have been recently established with a significance of 5σ [9] using the dominant $\omega \rightarrow \pi^+ \pi^- \pi^0$ decay, which has a branching fraction (\mathcal{B}) of $(89.2 \pm 0.7)\%$ [10]. Averaged with earlier measurements [11,12], $\mathcal{B}(\chi_{c1}(3872) \rightarrow \omega J/\psi) / \mathcal{B}(\chi_{c1}(3872) \rightarrow \pi^+ \pi^- J/\psi) = 1.4 \pm 0.3$. However, $\omega \rightarrow \pi^+ \pi^-$ decays, with $\mathcal{B}(\omega \rightarrow \pi^+ \pi^-) = (1.53 \pm 0.12)\%$ [10], are expected to contribute to the denominator at the 2% level if $\rho^0 - \omega$ interference is neglected. The interference can change this estimate by a

large factor. Therefore, an analysis of the $m_{\pi^+ \pi^-}$ spectrum is necessary to disentangle the ρ^0 and ω contributions. Such analyses were performed by the CDF [13] and the Belle [3] Collaborations, using the Breit–Wigner sum model, yielding inconclusive results due to the large statistical uncertainties.

In this paper, we report an analysis of a $B^+ \rightarrow K^+ \chi_{c1}(3872)$, $\chi_{c1}(3872) \rightarrow \pi^+ \pi^- J/\psi$, $J/\psi \rightarrow \mu^+ \mu^-$ data sample collected using the LHCb detector, with proton-proton (pp) collision energies of 7, 8 and 13 TeV, corresponding to a total integrated luminosity of 9 fb^{-1} . The inclusion of charge-conjugate processes is implied throughout. This sample is about 6 times more sensitive to an ω contribution than those used in Refs. [3,13]. The LHCb detector [14,15] is a single-arm forward spectrometer covering the pseudorapidity range $2 < \eta < 5$, designed for the study of particles containing b or c quarks. The detector elements that are particularly relevant to this analysis are: a silicon-strip vertex detector surrounding the pp interaction region that allows b hadrons to be identified from their characteristically long flight distance; a tracking system that provides a measurement of the momentum, p , of charged particles; two ring-imaging Cherenkov detectors that are able to discriminate between different species of charged hadrons and the muon detector.

The selection of $\chi_{c1}(3872) \rightarrow \pi^+ \pi^- J/\psi$ candidates is based on the reconstruction of $B^+ \rightarrow K^+ \pi^+ \pi^- J/\psi (\rightarrow \mu^+ \mu^-)$ decays, which provides for efficient background suppression and optimal dipion mass resolution. Both muon candidates are identified by the muon detector. The dimuon mass must be consistent with the known J/ψ mass [10], and all five final state particles must form a good-quality vertex significantly displaced from the closest primary pp interaction vertex (PV). The hadron candidate most likely to be a kaon is selected as the kaon candidate. Each hadron must have a significant impact parameter with respect to any PV. To remove multiple entries per event, the

*Full author list given at the end of the article.

B^+ candidate with the largest scalar sum of the hadron and J/ψ candidate transverse-momenta is selected. To improve mass resolution, the B^+ candidates are kinematically constrained to point to the closest PV and reproduce the known J/ψ mass [16]. The mass of these candidates must be consistent with the known B^+ mass [10], which is then also included among the kinematic constraints. The resulting $m_{\pi^+\pi^-J/\psi}$ distribution (Fig. 1) is fit with a signal (background) shape modeled by a double-sided Crystal Ball [17] (quadratic) function, yielding 6788 ± 117 $\chi_{c1}(3872) \rightarrow \pi^+\pi^-J/\psi$ decays with a $\chi_{c1}(3872)$ mass resolution of $\sigma_m = 2.66 \pm 0.09$ MeV (natural units are used throughout). The signal purity is 77% within $\pm 2\sigma_m$ around the $\chi_{c1}(3872)$ mass. The dominant source of background is from B^+ decays to J/ψ meson and excited kaons (K^{*+}), which decay to $K^+\pi^+\pi^-$. The dipion mass distribution is obtained by two-dimensional unbinned fits of the $\chi_{c1}(3872)$ signal yields to the $(m_{\pi^+\pi^-J/\psi}, m_{\pi^+\pi^-})$ data in $m_{\pi^+\pi^-}$ intervals. The signal shape in $m_{\pi^+\pi^-J/\psi}$ is fixed to the global fit result of Fig. 1, while the background shape may vary in each $m_{\pi^+\pi^-}$ interval. The signal and the background $m_{\pi^+\pi^-J/\psi}$ shapes are then multiplied by a two-body phase-space factor, i.e. the J/ψ momentum in the $\chi_{c1}(3872)$ rest frame ($p_{J/\psi}$), which depends on both $m_{\pi^+\pi^-J/\psi}$ and $m_{\pi^+\pi^-}$. The resultant shapes are normalized to unity using their integral over the fitted phase-space range. The obtained data points are shown in Fig. 2.

Signal simulation is used to obtain the $m_{\pi^+\pi^-}$ dependence of the dipion mass resolution and of the reconstruction efficiency. In the simulation, pp collisions are generated using PYTHIA [18,19] with a specific LHCb configuration [20]. Decays of unstable particles are described by EvtGen [21], in which final-state radiation is generated using PHOTOS [22]. In particular, $B^+ \rightarrow K^+\chi_{c1}(3872)$, $\chi_{c1}(3872) \rightarrow J/\psi\rho^0$, $\rho^0 \rightarrow \pi^+\pi^-$, $J/\psi \rightarrow \mu^+\mu^-$ signal decays are simulated using the helicity model where the $\chi_{c1}(3872)$ decays via an S -wave, which

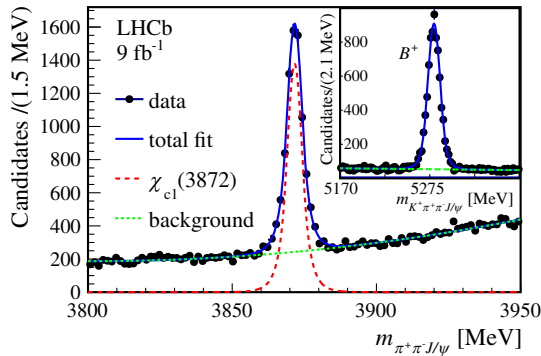


FIG. 1. Distribution of $m_{\pi^+\pi^-J/\psi}$ [$m_{K^+\pi^+\pi^-J/\psi}$ in the inset] from $B^+ \rightarrow K^+\pi^+\pi^-J/\psi$ candidates within $\pm 2\sigma$ around the B^+ [$\chi_{c1}(3872)$] mass, overlaid with the fit including the total (solid blue), signal (dashed red), and background (dashed green) components.

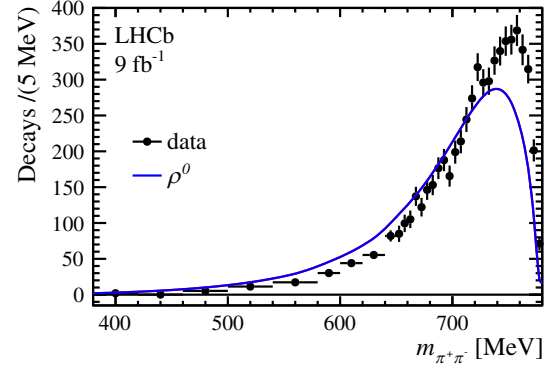


FIG. 2. Distribution of $m_{\pi^+\pi^-}$ in $\chi_{c1}(3872) \rightarrow \pi^+\pi^-J/\psi$ decays, fit with the ρ^0 -only model.

describes the angular distributions in the data well [5]. When integrating over $m_{\pi^+\pi^-}$, the generated $m_{\pi^+\pi^-}$ distribution is weighted to reproduce the observed distribution. The interaction of the generated particles with the detector, and its response, are implemented using the Geant4 toolkit [23,24] as described in Ref. [25]. The underlying pp interaction is reused multiple times, with an independently generated signal decay for each event [26]. The transverse-momentum distribution of the signal B^+ is weighted to match the data. The relative signal reconstruction efficiency obtained from the simulation is well described by a quadratic function, $\epsilon(m_{\pi^+\pi^-}) = 0.966 + 1.345 \times 10^{-3}(m_{\pi^+\pi^-} - 700) + 1.607 \times 10^{-6}(m_{\pi^+\pi^-} - 700)^2$, and the dipion mass resolution by $\sigma(m_{\pi^+\pi^-}) = 2.39(1 - \exp(-m_{\pi^+\pi^-}/220.3)) - 5.4 \exp(-m_{\pi^+\pi^-}/220.3)$, where $m_{\pi^+\pi^-}$ and $\sigma(m_{\pi^+\pi^-})$ are in MeV. The simulation underestimates the $\chi_{c1}(3872)$ and B^+ mass resolution by 6% and 14%, respectively. Therefore, $\sigma(m_{\pi^+\pi^-})$ is scaled up by $f_m = 1.06$, which is varied from 1.00 to 1.14 to assess a systematic uncertainty. All theoretical probability density functions fit to the data, $\mathcal{P}(m_{\pi^+\pi^-})$, are multiplied by the relative efficiency function, $\epsilon(m_{\pi^+\pi^-})$ and convolved with a Gaussian distribution characterized by a root-mean-square value of $f_m\sigma(m_{\pi^+\pi^-})$.

The matrix element, \mathcal{M} , describing the three-body decay, $\chi_{c1}(3872) \rightarrow \pi^+\pi^-J/\psi$, is related to $\mathcal{P}(m_{\pi^+\pi^-})$ via a scaling (S) and the phase-space factors, $\mathcal{P}(m_{\pi^+\pi^-}) = Sp_{J/\psi}p_\pi|\mathcal{M}|^2$, where p_π is the pion momentum in the rest frame of the $\pi^+\pi^-$ system. The scaling factor S is a nuisance parameter.

Following the previous analyses [3,13], the ρ^0 component is first parametrized as a Breit–Wigner (BW) amplitude,

$$\mathcal{M} = \text{BW}(s|m_\rho, \Gamma_\rho) = \frac{m_\rho \Gamma_\rho \sqrt{B_1(p_\pi)/B_1(p_\pi^\rho)}}{m_\rho^2 - s - im_\rho \Gamma(s)},$$

$$\Gamma(s) = \Gamma_\rho \frac{p_\pi m_\rho B_1(p_\pi)}{p_\pi^\rho \sqrt{s} B_1(p_\pi^\rho)}, \quad (1)$$

where $s \equiv m_{\pi^+\pi^-}^2$, $p_\pi^\rho = p_\pi(m_\rho)$, $m_\rho = 775.26$ MeV, $\Gamma_\rho = 147.4$ MeV [10], and $B_1(p) = p^2/[(1 + (Rp)^2)]$ is the

Blatt–Weisskopf barrier factor for the P -wave decay of a vector particle to $\pi^+\pi^-$ and contains an effective hadron-size parameter R . With R adjusted to 1.45 GeV^{-1} , a complex phase of the BW amplitude varies in the fitted $m_{\pi^+\pi^-}$ range within 1 degree of the isovector $\pi^+\pi^-$ P -wave parametrization extracted from the scattering data by the phenomenological analysis of Ref. [27]. A similar value of 1.5 GeV^{-1} was used in the previous analyses [3,13]. The χ^2 fit, with S as the only fit parameter, fails to describe the data as shown in Fig. 2, with a χ^2 value per number of degrees of freedom ($\chi^2/n.d.o.f.$) equal to $366.6/34$. A large disagreement between the data and the $\chi_{c1}(3872) \rightarrow \rho^0 J/\psi$ amplitude at high dipion masses was missed in the previous comparisons with the $\chi_{c1}(3872) \rightarrow \rho^0 J/\psi$ simulation (see Fig. S2 in the Supplemental Material of Ref. [5]; see also Refs. [28,29]), because the EvtGen [21] model does not correctly simulate the impact of the phase-space factors (here $p_{J/\psi} p_\pi$) on resonant shapes. As a consequence, the large $\rho^0 - \omega$ interference in the data (see below) was mistakenly interpreted as a part of the ρ^0 resonance itself.

Adding an ω contribution via the BW sum model with $\mathcal{M} = \text{BW}(s|m_\rho, \Gamma_\rho) + a \exp(i\phi) \text{BW}(s|m_\omega, \Gamma_\omega)$, where a and ϕ are the amplitude and phase of the ω component relative to the ρ^0 term [3,13], improves the fit quality substantially, $\chi^2/n.d.o.f. = 102.9/33$, yet not enough to be acceptable. Summing BW amplitudes results in matrix elements that are not unitary, violating first principles of scattering theory. A two-channel K -matrix (K) model [30], coupling the $\pi^+\pi^-$ and $\pi^+\pi^-\pi^0$ channels via an ω contribution, resolves this issue,

$$K = \frac{1}{m_\rho^2 - s} \begin{pmatrix} g_{\rho \rightarrow 2\pi}^2 & 0 \\ 0 & 0 \end{pmatrix} + \frac{1}{m_\omega^2 - s} \begin{pmatrix} g_{\omega \rightarrow 2\pi}^2 & g_{\omega \rightarrow 2\pi} g_{\omega \rightarrow 3\pi} \\ g_{\omega \rightarrow 2\pi} g_{\omega \rightarrow 3\pi} & g_{\omega \rightarrow 3\pi}^2 \end{pmatrix}, \quad (2)$$

where g are the coupling constants described later. The $g_{\rho \rightarrow 3\pi}^2$ coupling is 4–5 orders of magnitude smaller than $g_{\rho \rightarrow 2\pi}^2$ [10,31,32] and has been neglected here. The T -matrix is obtained from $\hat{T} = [1 - iK\varrho]^{-1}K$, where the phase-space matrix ϱ is diagonal, $\varrho = \text{diag}(\varrho_{2\pi}(s), \varrho_{3\pi}(s))$ and is detailed in the Supplemental Material [33]. The decay amplitude is given by

$$\mathcal{M} = \hat{A}_{2\pi} \sqrt{B_1(p_\pi)}, \quad (3)$$

where $\hat{A}_{2\pi} \equiv \alpha_{2\pi} \hat{T}_{2\pi,2\pi} + \alpha_{3\pi} \hat{T}_{2\pi,3\pi}$, and the elements of the production Q -vector ($\alpha_{2\pi}$, $\alpha_{3\pi}$) are real [34]. The coupling constants are fully determined from other experiments [10],

$$g_{\rho \rightarrow 2\pi}^2 = m_\rho \Gamma_\rho / \varrho_{2\pi}(m_\rho^2), \quad (4)$$

$$g_{\omega \rightarrow 3\pi}^2 = m_\omega \Gamma_\omega \mathcal{B}(\omega \rightarrow \pi^+\pi^-\pi^0) / \varrho_{3\pi}(m_\omega^2), \quad (5)$$

$$g_{\omega \rightarrow 2\pi}^2 = m_\omega \Gamma_\omega \mathcal{B}(\omega \rightarrow \pi^+\pi^-) / \varrho_{2\pi}(m_\omega^2). \quad (6)$$

Numerically, $g_{\omega \rightarrow 2\pi}^2 / g_{\rho \rightarrow 2\pi}^2 \approx 0.0009$, while $g_{\omega \rightarrow 2\pi} g_{\omega \rightarrow 3\pi} / g_{\rho \rightarrow 2\pi}^2 \approx 0.01$. Thus, the diagonal ω coupling to two pions can be neglected in comparison with the off diagonal coupling. In this approximation, equivalent to the full formalism given the precision of this analysis,

$$\hat{T}_{2\pi,2\pi} \approx \frac{g_{\rho \rightarrow 2\pi}^2}{m_\rho^2 - s - i g_{\rho \rightarrow 2\pi}^2 \varrho_{2\pi}(s)}, \quad (7)$$

which is the ρ^0 Breit-Wigner amplitude [Eq. (1)] and $\alpha_{2\pi}$ is the ρ^0 production factor in the $\chi_{c1}(3872)$ decay. A mild dependence of $\alpha_{2\pi}$ on s is possible, since $\alpha_{2\pi}(s)$ must be analytic and cannot change much within the resonance widths (see e.g. Ref. [35]). Using Chebyshev polynomials (C_n) to express the dependence: $\alpha_{2\pi}(s) = \sum_{n=0}^{N-1} P_n C_n(\hat{s})$, where $\hat{s} \equiv 2(s - s_{\min}) / (s_{\max} - s_{\min}) - 1$, $s_{\min} = (380 \text{ MeV})^2$, and $s_{\max} = (775 \text{ MeV})^2$. The polynomial coefficients P_n are determined from a fit to the data, except for P_0 , which is set to unity as the normalization choice. For $\alpha_{2\pi}(s)$ to have the expected theoretical behavior, the series must converge, $|P_{n+1}| < |P_n|$, and N should be kept small.

The ω contribution enters via the element,

$$\hat{T}_{2\pi,3\pi} \approx \frac{g_{\omega \rightarrow 2\pi} g_{\omega \rightarrow 3\pi} (m_\rho^2 - s)}{(m_\rho^2 - s - i g_{\rho \rightarrow 2\pi}^2 \varrho_{2\pi}(s)) (m_\omega^2 - s - i g_{\omega \rightarrow 3\pi}^2 \varrho_{3\pi}(s))}. \quad (8)$$

This term approaches zero at the bare ρ^0 pole mass, which complicates probing the ω contribution, $m_\omega = 782.66 \pm 0.13 \text{ MeV}$ and $\Gamma_\omega = 8.68 \pm 0.13 \text{ MeV}$ [10]. This zero is an artifact of the K -matrix approach, rather than an expectation from scattering theory. To remove it and restore a more physical behavior of the ω term,

$$\alpha_{3\pi} = a_\omega \frac{m_\omega^2 - m_\rho^2}{m_\rho^2 - s}, \quad (9)$$

is set. The constant term $m_\omega^2 - m_\rho^2$ is introduced above to make a_ω express the ratio of ω/ρ amplitudes at the ω pole. The value of a_ω is determined by the fit to the data. Using Eqs. (7)–(9), with $\alpha_{2\pi}$ constant ($N = 0$), is the common method to describe $\rho^0 - \omega$ interference in analyses of the $\pi^+\pi^-$ system [36]. The exact K -matrix formulas are used here. In view of Eq. (7), models with $\alpha_{3\pi} = 0$ are interpreted as containing a ρ^0 component only. The following integrals are calculated to quantify a relative rate of the ω

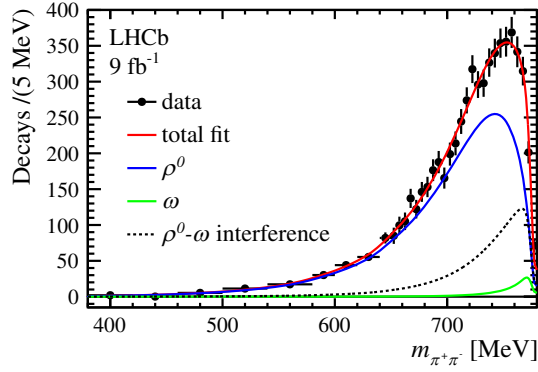


FIG. 3. Distribution of $m_{\pi^+\pi^-}$ in $\chi_{c1}(3872) \rightarrow \pi^+\pi^-J/\psi$ decays, fit with the default K -matrix model.

contribution: $I_{\text{tot}} = \int \mathcal{P}(m_{\pi^+\pi^-}) dm_{\pi^+\pi^-}$, $I_\rho = \int \mathcal{P}(m_{\pi^+\pi^-} | \alpha_{3\pi} = 0) dm_{\pi^+\pi^-}$, and $I_\omega = \int \mathcal{P}(m_{\pi^+\pi^-} | \alpha_{2\pi} = 0) dm_{\pi^+\pi^-}$, where $\mathcal{P}(m_{\pi^+\pi^-})$ is neither convolved with the mass resolution, nor multiplied by the efficiency function. The integration is performed over the full phase space. To quantify the overall impact of ω on the total rate, including $\rho^0 - \omega$ interference effects, the ratio $\mathcal{R}_\omega^{\text{all}} \equiv 1 - I_\rho/I_{\text{tot}}$ is defined. The traditional ω fit fraction is given by $\mathcal{R}_\omega^0 \equiv I_\omega/I_{\text{tot}}$. Finally, to probe the ratio of the $\chi_{c1}(3872)$ isospin conserving to isospin violating couplings, the ratio $\mathcal{R}_{\omega/\rho}^0 \equiv I_\omega/I_\rho$ is introduced. Using the $B^+ \rightarrow K^+\chi_{c1}(3872)$ simulation, the extraction of the dipion mass distribution and subsequent fit with the K -matrix model, with the efficiency and the mass resolution corrections included, are verified to

a precision an order of magnitude better than the total systematic uncertainties reported below.

Allowing the ω term in the K -matrix model with the constant $\alpha_{2\pi}$ improves the fit quality to $\chi^2/n.d.o.f. = 55.1/33$, resulting in a significance for the ω contribution of $n_\sigma = (\chi_{a_\omega=0}^2 - \chi_{a_\omega \neq 0}^2)^{1/2} = 17.7\sigma$ [37]. However, the p -value of the fit is marginal (0.9%). Introducing a term linear in s to $\alpha_{2\pi}(s)$ improves the fit with $\chi^2/n.d.o.f. = 24.7/32$, p -value = 82%, and a small slope coefficient, $P_1 = 0.23 \pm 0.05$. This fit, shown in Fig. 3, is taken as the default model and yields $n_\sigma = 8.1\sigma$, $\mathcal{R}_\omega^{\text{all}} = 0.214 \pm 0.023$, $\mathcal{R}_\omega^0 = 0.0193 \pm 0.0044$, $\mathcal{R}_{\omega/\rho}^0 = 0.0246 \pm 0.0062$, and $a_\omega = 0.208 \pm 0.024$. The ω contribution is at the level of $\mathcal{R}_\omega^0 \approx 2\%$ as expected from the $\chi_{c1}(3872) \rightarrow \omega J/\psi$, $\omega \rightarrow \pi^+\pi^-\pi^0$ measurements (see above). The impact on the overall $\chi_{c1}(3872) \rightarrow \pi^+\pi^-J/\psi$ rate given by $\mathcal{R}_\omega^{\text{all}}$ is an order of magnitude larger, enhanced by the $\rho^0 - \omega$ interference. Allowing a quadratic term in $\alpha_{2\pi}(s)$ lowers the p -value of the fit to 78% with $\chi^2/n.d.o.f. = 24.6/31$, indicating that too much freedom is added to the model. The P_2 coefficient is small and consistent with zero, $P_2 = 0.016 \pm 0.047$, while all other fit results remain consistent with the default fit, $P_1 = 0.21 \pm 0.07$, $\mathcal{R}_\omega^{\text{all}} = 0.206 \pm 0.035$, $\mathcal{R}_\omega^0 = 0.0178 \pm 0.0062$, $\mathcal{R}_{\omega/\rho}^0 = 0.0225 \pm 0.088$, and $a_\omega = 0.197 \pm 0.042$. The significance of the ω contribution remains very high, $n_\sigma = 5.5\sigma$ and is now underestimated, since the null hypothesis ($a_\omega = 0$) gives an unphysical polynomial correction (the quadratic term,

TABLE I. Results for ω fractions with systematic uncertainties. See text for a description of the individual entries.

Fit type	$\chi^2/n.d.o.f.$	p -value	$\mathcal{R}_\omega^{\text{all}}$	\mathcal{R}_ω^0	$\mathcal{R}_{\omega/\rho}^0$	n_σ
Default	24.7/32	0.82	0.214 ± 0.023	0.019 ± 0.004	0.025 ± 0.006	8.1σ
$P_2 \neq 0$	24.6/31	0.78	0.206 ± 0.035	0.018 ± 0.006	0.023 ± 0.009	5.5σ
Gaussian $\chi_{c1}(3872)$	20.0/32	0.95	0.194 ± 0.024	0.016 ± 0.004	0.020 ± 0.006	7.3σ
cubic $\epsilon(m_{\pi^+\pi^-})$	24.5/32	0.83	0.221 ± 0.023	0.021 ± 0.005	0.027 ± 0.007	8.1σ
had.ID corrections	24.6/32	0.82	0.214 ± 0.023	0.019 ± 0.004	0.025 ± 0.006	8.1σ
BDT selection	24.6/32	0.82	0.207 ± 0.022	0.018 ± 0.004	0.023 ± 0.006	7.9σ
$\sigma(m_{\pi^+\pi^-}) \times 1.0$	26.6/32	0.74	0.213 ± 0.023	0.019 ± 0.004	0.025 ± 0.006	8.1σ
$\sigma(m_{\pi^+\pi^-}) \times 1.14$	22.6/32	0.89	0.215 ± 0.023	0.020 ± 0.004	0.026 ± 0.006	8.1σ
$m_{\pi^+\pi^-} < 775$ MeV	18.0/31	0.97	0.196 ± 0.024	0.016 ± 0.004	0.021 ± 0.006	7.1σ
$\cos\theta_X < 0$	26.9/32	0.72	0.211 ± 0.035	0.019 ± 0.007	0.024 ± 0.010	5.2σ
$\cos\theta_X > 0$	42.2/32	0.11	0.217 ± 0.030	0.021 ± 0.006	0.027 ± 0.009	4.2σ
NR production of 2π	24.7/32	0.82	0.214 ± 0.022	0.019 ± 0.004	0.025 ± 0.006	8.1σ
D -wave free	24.5/31	0.79	0.210 ± 0.029	0.017 ± 0.005	0.021 ± 0.007	7.8σ
D -wave fixed at 4%	24.5/32	0.82	0.208 ± 0.023	0.018 ± 0.004	0.023 ± 0.006	7.9σ
ρ'	25.1/32	0.80	0.209 ± 0.023	0.018 ± 0.004	0.024 ± 0.006	8.1σ
$R_{\text{prod}} = 0$ GeV $^{-1}$	24.7/32	0.82	0.209 ± 0.023	0.019 ± 0.004	0.024 ± 0.006	7.9σ
$R_{\text{prod}} = 30$ GeV $^{-1}$	24.6/32	0.82	0.229 ± 0.022	0.021 ± 0.004	0.028 ± 0.006	8.7σ
$R = 1.3$ GeV $^{-1}$	24.7/32	0.82	0.216 ± 0.022	0.020 ± 0.004	0.026 ± 0.006	8.2σ
$R = 1.6$ GeV $^{-1}$	24.7/32	0.82	0.212 ± 0.023	0.019 ± 0.004	0.025 ± 0.006	8.0σ
GS model	24.8/32	0.81	0.221 ± 0.024	0.021 ± 0.005	0.028 ± 0.007	7.8σ
Summary			$0.214 \pm 0.023 \pm 0.020$	$0.019 \pm 0.004 \pm 0.003$	$0.025 \pm 0.006 \pm 0.005$	$> 7.1\sigma$

$P_2 = 0.17 \pm 0.02$, comparable to, and more significant than the linear term, $P_1 = 0.16 \pm 0.05$.

A number of analysis variations have been performed to evaluate systematic uncertainties on the ω fraction, as summarized in Table I. In the dipion mass extraction from the data, Gaussian functions are used for the $\chi_{c1}(3872)$ shape in $m_{\pi^+\pi^-J/\psi}$ data, rather than Crystal Ball functions. A cubic polynomial replaces the quadratic function in the relative efficiency parametrization.

Data-driven corrections to the simulation of the hadron identification are implemented, as a cross-check. To check further the relative efficiency simulation and the background subtraction, a tighter data selection is implemented with a Boosted Decision Tree (BDT) classifier [38], using inputs from hadron identification variables, the B^+ vertex quality, the PV impact parameters of the final-state particles and the B^+ candidate, the hadron transverse-momenta and the B^+ flight distance. The tighter selection reduces the combinatoric background under the B^+ peak in the $m_{K^+\pi^+\pi^-J/\psi}$ distribution from 9.4% to 3.1%, resulting in an overall background reduction under the $\chi_{c1}(3872)$ peak in the $m_{\pi^+\pi^-J/\psi}$ distribution from 23% to 17%. At the same time, the $\chi_{c1}(3872)$ signal yield is reduced by only 0.4%.

To evaluate uncertainties due to the mass resolution used in the fit, the scaling factor f_m is varied and the fit range is reduced to exclude the last interval of the $m_{\pi^+\pi^-}$ distribution (775–780 MeV), since this falls beyond the phase-space limit, and therefore its content is very sensitive to $\sigma(m_{\pi^+\pi^-})$.

To check for interference effects between $B^+ \rightarrow K^+\chi_{c1}(3872)$ and $B^+ \rightarrow K^{*+}J/\psi$ decays, the data are split into two subsamples depending on the sign of $\cos\theta_X$, where θ_X is the $\chi_{c1}(3872)$ helicity angle, the angle between the K^+ and J/ψ momenta in the $\chi_{c1}(3872)$ rest frame. The composition of K^{*+} resonances is different in each subsample.

As a variation of the production model, nonresonant (NR) terms are added to the production vector, $(\hat{A}_{2\pi}, \hat{A}_{3\pi}) = [1 - iK\rho]^{-1}[K(\alpha_{2\pi}, \alpha_{3\pi}) + (f_{2\pi}, f_{3\pi})]$. Without $\chi_{c1}(3872) \rightarrow 3\pi J/\psi$ data in the fit, the NR production parameter $f_{3\pi}$ cannot be probed, thus it is set to zero. A good-quality fit is obtained with constant $\alpha_{2\pi}$, which gives $f_{2\pi} = (-9.7 \pm 1.6) \times 10^{-7}$.

The default fit assumes an S -wave $\chi_{c1}(3872)$ decay. When a D -wave component is allowed in the fit, multiplying $|\mathcal{M}|^2$ by $1 + A_D^2 B_2(p_{J/\psi})/B_2(p_{J/\psi}^0)$, where $p_{J/\psi}^0 \equiv p_{J/\psi}(m_\rho)$ and $B_2(p) \equiv p^4/(9 + 3(Rp)^2 + (Rp)^4)$, the A_D parameter is consistent with zero, 0.13 ± 0.41 . Tuning A_D to 0.176 produces a 4% D -wave fraction, equal to the upper limit from studies of the angular correlations [5].

Since the hadron size parameter R is tuned to the scattering data, which automatically includes any ρ^0 excitations, there is no strong motivation to include the $\rho(1450)$ pole [10] (ρ') in the K -matrix model. When included, the fit quality is slightly reduced.

The size parameter R used in $B_1(p_\pi)$ of Eq. (3) could be related to the $\chi_{c1}(3872)$ size, rather than the ρ^0 or ω sizes. Thus, fit variations are tried in which it has an independent value, R_{prod} , varied from zero to 30 GeV $^{-1}$. The R value itself is varied within the range 1.3–1.6 GeV $^{-1}$. An alternative model of the ρ^0 shape, that does not include an R -dependent Blatt-Weisskopf form factor, is provided by the Gounaris-Sakurai (GS) formula [39], and was utilized by the *BABAR* Collaboration to describe high statistics $e^+e^- \rightarrow \pi^+\pi^-(\gamma)$ data [40]. As discussed in the Supplemental Material [33], when applying this prescription with ρ^0 , ρ' and ω contributions, an excellent fit to the data is obtained, $\chi^2/n.d.o.f. = 24.8/32$, p -value = 81%, matching the fit quality of the default fit.

Total systematic uncertainties, given at the bottom of Table I, are set to cover the maximal deviation from the default fit results, and are comparable to the statistical uncertainties. The lowest ω significance is 7.1σ , excluding the subsamples and $P_2 \neq 0$ fit as discussed above. This is a more significant observation of $\chi_{c1}(3872) \rightarrow \omega J/\psi$ decays than achieved using the dominant $\omega \rightarrow \pi^+\pi^-\pi^0$ decay channel.

In addition to the resonant coupling constants, the limited phase space in $\chi_{c1}(3872) \rightarrow \pi^+\pi^-J/\psi$ decays has a large impact on the $\mathcal{R}_{\omega/\rho}^0$ value capturing a much smaller fraction of the ω resonance than for the ρ^0 resonance. To probe the resonant coupling constants, the phase space can be artificially extended to contain both resonance peaks by setting $m_{\chi_{c1}(3872)} = 4000$ MeV, as illustrated in the Supplemental Material [33]. Integrating the default $\mathcal{P}(m_{\pi^+\pi^-})$ model in the extended phase space, $\mathcal{R}_{\omega/\rho}^0 = 0.18 \pm 0.05$ is obtained and then used to deduce the ratio of the isospin violating to isospin conserving $\chi_{c1}(3872)$ couplings,

$$\frac{g_{\chi_{c1}(3872) \rightarrow \rho^0 J/\psi}}{g_{\chi_{c1}(3872) \rightarrow \omega J/\psi}} = \sqrt{\frac{\mathcal{B}(\omega \rightarrow \pi^+\pi^-)}{\mathcal{R}_{\omega/\rho}^0}} = 0.29 \pm 0.04.$$

This value is an order of magnitude larger than expected for pure $c\bar{c}$ states, as exemplified by the corresponding value for the $\psi(2S)$ state [10],

$$\begin{aligned} \frac{g_{\psi(2S) \rightarrow \pi^0 J/\psi}}{g_{\psi(2S) \rightarrow \eta J/\psi}} &= \sqrt{\frac{\mathcal{B}(\psi(2S) \rightarrow \pi^0 J/\psi) p_\eta^3}{\mathcal{B}(\psi(2S) \rightarrow \eta J/\psi) p_{\pi^0}^3}} \\ &= 0.045 \pm 0.001, \end{aligned}$$

where p_η and p_{π^0} are the breakup momenta [41]. Therefore, the $\chi_{c1}(3872)$ state cannot be a pure charmonium state. Large isospin violation is naturally expected in models in which the $\chi_{c1}(3872)$ state has a significant $D\bar{D}^*$ component, either as constituents (i.e. in the ‘‘molecular model’’)

or generated dynamically in the decay [42–51]. The proximity of the $\chi_{c1}(3872)$ mass to the $D^0\bar{D}^{*0}$ threshold, enhances such contributions over D^+D^{*-} combinations, which are 8 MeV heavier. It has also been suggested in compact tetraquark models that two neutral states could be degenerate and mix, giving rise to large isospin violation in $\chi_{c1}(3872)$ decays [52–54].

In summary, the ρ^0 and ω contributions to $\chi_{c1}(3872) \rightarrow \pi^+\pi^-J/\psi$ decays are resolved for the first time using a much larger data sample than previously available. Through $\rho^0 - \omega$ interference, the ω contribution accounts for $(21.4 \pm 2.3 \pm 2.0)\%$ of the total rate, or equivalently, $\mathcal{B}(\chi_{c1}(3872) \rightarrow \rho^0 J/\psi)/\mathcal{B}(\chi_{c1}(3872) \rightarrow \pi^+\pi^-J/\psi) = (78.6 \pm 2.3 \pm 2.0)\%$. Excluding interference effects, the ω contribution, $(1.9 \pm 0.4 \pm 0.3)\%$, is found to be consistent with, but more precise than the previous $\chi_{c1}(3872) \rightarrow \omega J/\psi$ measurements utilizing $\omega \rightarrow \pi^+\pi^-\pi^0$ decays [9,11,12]. The isospin violating ρ^0 contribution, quantified for the first time with proper subtraction of the ω contribution, is an order of magnitude too large for $\chi_{c1}(3872)$ to be a pure charmonium state.

This analysis also serves as an excellent illustration for why a simple sum of ρ^0 and ω Breit-Wigner amplitudes should not be used to describe interfering resonances. Such a model fails to describe the data, while the K -matrix approach, which respects unitarity, provides an excellent description of the data and gives numerical results that are consistent with the previous $\chi_{c1}(3872) \rightarrow \omega J/\psi$ measurements utilizing $\omega \rightarrow \pi^+\pi^-\pi^0$ decays.

We express our gratitude to our colleagues in the CERN accelerator departments for the excellent performance of the LHC. We thank the technical and administrative staff at the LHCb institutes. We acknowledge support from CERN and from the national agencies: CAPES, CNPq, FAPERJ, and FINEP (Brazil); MOST and NSFC (China); CNRS/IN2P3 (France); BMBF, DFG and MPG (Germany); INFN (Italy); NWO (Netherlands); MNiSW and NCN (Poland); MEN/IFA (Romania); MICINN (Spain); SNSF and SER (Switzerland); NASU (Ukraine); STFC (United Kingdom); DOE NP and NSF (USA). We acknowledge the computing resources that are provided by CERN, IN2P3 (France), KIT and DESY (Germany), INFN (Italy), SURF (Netherlands), PIC (Spain), GridPP (United Kingdom), CSCS (Switzerland), IFIN-HH (Romania), CBPF (Brazil), Polish WLCG (Poland) and NERSC (USA). We are indebted to the communities behind the multiple open-source software packages on which we depend. Individual groups or members have received support from ARC and ARDC (Australia); Minciencias (Colombia); AvH Foundation (Germany); EPLANET, Marie Skłodowska-Curie Actions and ERC (European Union); A*MIDEX, ANR, IPhU and Labex P2IO, and Région Auvergne-Rhône-Alpes (France); Key Research Program of Frontier Sciences of CAS, CAS PIFI, CAS CCEPP, Fundamental Research Funds for the Central Universities, and Sci. and Tech. Program of Guangzhou (China); MEFP, GVA, XuntaGal, GENCAT and Prog. Atracción Talento, CM (Spain); SRC (Sweden); the Leverhulme Trust, the Royal Society and UKRI (United Kingdom).

-
- [1] S. K. Choi *et al.* (Belle Collaboration), *Phys. Rev. Lett.* **91**, 262001 (2003).
- [2] B. Aubert *et al.* (BABAR Collaboration), *Phys. Rev. D* **71**, 031501 (2005).
- [3] S. K. Choi *et al.* (Belle Collaboration), *Phys. Rev. D* **84**, 052004 (2011).
- [4] R. Aaij *et al.* (LHCb Collaboration), *Phys. Rev. Lett.* **110**, 222001 (2013).
- [5] R. Aaij *et al.* (LHCb Collaboration), *Phys. Rev. D* **92**, 011102(R) (2015) and supplementary material at <https://cds.cern.ch/record/2012165/files/>.
- [6] E. Eichten, K. Gottfried, T. Kinoshita, K. D. Lane, and T.-M. Yan, *Phys. Rev. D* **17**, 3090 (1978); **21**, 313(E) (1980).
- [7] S. L. Olsen, T. Skwarnicki, and D. Zieminska, *Rev. Mod. Phys.* **90**, 015003 (2018).
- [8] F.-K. Guo, C. Hanhart, U.-G. Meißner, Q. Wang, Q. Zhao, and B.-S. Zou, *Rev. Mod. Phys.* **90**, 015004 (2018).
- [9] M. Ablikim *et al.* (BESIII Collaboration), *Phys. Rev. Lett.* **122**, 232002 (2019).
- [10] P. A. Zyla *et al.* (Particle Data Group), *Prog. Theor. Exp. Phys.* **2020**, 083C01 (2020).
- [11] K. Abe *et al.* (Belle Collaboration), [arXiv:hep-ex/0505037](https://arxiv.org/abs/hep-ex/0505037).
- [12] P. del Amo Sanchez *et al.* (BABAR Collaboration), *Phys. Rev. D* **82**, 011101 (2010).
- [13] A. Abulencia *et al.* (CDF Collaboration), *Phys. Rev. Lett.* **96**, 102002 (2006).
- [14] A. A. Alves, Jr. *et al.* (LHCb Collaboration), *J. Instrum.* **3**, S08005 (2008).
- [15] LHCb Collaboration, *Int. J. Mod. Phys. A* **30**, 1530022 (2015).
- [16] W. D. Hulsbergen, *Nucl. Instrum. Methods Phys. Res., Sect. A* **552**, 566 (2005).
- [17] T. Skwarnicki, Ph.D. thesis, Institute of Nuclear Physics, Krakow, 1986 [Report No. DESY-F31-86-02].
- [18] T. Sjöstrand, S. Mrenna, and P. Skands, *Comput. Phys. Commun.* **178**, 852 (2008).
- [19] T. Sjöstrand, S. Mrenna, and P. Skands, *J. High Energy Phys.* **05** (2006) 026.
- [20] I. Belyaev *et al.*, *J. Phys. Conf. Ser.* **331**, 032047 (2011).
- [21] D. J. Lange, *Nucl. Instrum. Methods Phys. Res., Sect. A* **462**, 152 (2001).

- [22] N. Davidson, T. Przedzinski, and Z. Was, *Comput. Phys. Commun.* **199**, 86 (2016).
- [23] J. Allison, K. Amako, J. Apostolakis, H. Araujo, P. Dubois *et al.* (Geant4 Collaboration), *IEEE Trans. Nucl. Sci.* **53**, 270 (2006).
- [24] S. Agostinelli *et al.* (Geant4 Collaboration), *Nucl. Instrum. Methods Phys. Res., Sect. A* **506**, 250 (2003).
- [25] M. Clemencic, G. Corti, S. Easo, C. R. Jones, S. Miglioranza, M. Pappagallo, and P. Robbe, *J. Phys. Conf. Ser.* **331**, 032023 (2011).
- [26] D. Müller, M. Clemencic, G. Corti, and M. Gersabeck, *Eur. Phys. J. C* **78**, 1009 (2018).
- [27] R. Garcia-Martin, R. Kaminski, J. R. Pelaez, J. Ruiz de Elvira, and F. J. Yndurain, *Phys. Rev. D* **83**, 074004 (2011).
- [28] S. Chatrchyan *et al.* (CMS Collaboration), *J. High Energy Phys.* **04** (2013) 154.
- [29] M. Aaboud *et al.* (ATLAS Collaboration), *J. High Energy Phys.* **01** (2017) 117.
- [30] I. J. R. Aitchison, *Nucl. Phys.* **A189**, 417 (1972).
- [31] M. N. Achasov *et al.*, *Phys. Rev. D* **68**, 052006 (2003).
- [32] M. Benayoun, P. David, L. DelBuono, and O. Leitner, *Eur. Phys. J. C* **65**, 211 (2010).
- [33] See Supplemental Material at <http://link.aps.org/supplemental/10.1103/PhysRevD.108.L011103> for the K-matrix phase-space matrix elements, for details of the study with Gounaris-Sakurai resonant shape, and for extrapolation of the fitted amplitudes beyond the phase space limit.
- [34] S. U. Chung, J. Brose, R. Hackmann, E. Klempt, S. Spanier, and C. Strassburger, *Ann. Phys. (N.Y.)* **4**, 404 (1995).
- [35] A. Jackura *et al.* (JPAC/COMPASS Collaboration), *Phys. Lett. B* **779**, 464 (2018).
- [36] A. S. Goldhaber, G. C. Fox, and C. Quigg, *Phys. Lett.* **30B**, 249 (1969).
- [37] S. S. Wilks, *Ann. Math. Stat.* **9**, 60 (1938).
- [38] H. Voss, A. Hoecker, J. Stelzer, and F. Tegenfeldt, *Proc. Sci. ACAT2007* (2007) 040.
- [39] G. J. Gounaris and J. J. Sakurai, *Phys. Rev. Lett.* **21**, 244 (1968).
- [40] J. P. Lees *et al.* (BABAR Collaboration), *Phys. Rev. D* **86**, 032013 (2012).
- [41] C. Hanhart, Y. Kalashnikova, A. Kudryavtsev, and A. Nefediev, *Phys. Rev. D* **85**, 011501 (2012).
- [42] N. A. Törnqvist, *arXiv:hep-ph/0308277*.
- [43] N. A. Törnqvist, *Phys. Lett. B* **590**, 209 (2004).
- [44] M. B. Voloshin, *Phys. Lett. B* **579**, 316 (2004).
- [45] E. S. Swanson, *Phys. Lett. B* **588**, 189 (2004).
- [46] M. Suzuki, *Phys. Rev. D* **72**, 114013 (2005).
- [47] S. Coito, G. Rupp, and E. van Beveren, *Eur. Phys. J. C* **71**, 1762 (2011).
- [48] N. Li and S.-L. Zhu, *Phys. Rev. D* **86**, 074022 (2012).
- [49] S. Takeuchi, K. Shimizu, and M. Takizawa, *Prog. Theor. Exp. Phys.* **2014**, 123D01 (2014); **2015**, 079203(E) (2015).
- [50] Q. Wu, D.-Y. Chen, and T. Matsuki, *Eur. Phys. J. C* **81**, 193 (2021).
- [51] L. Meng, G.-J. Wang, B. Wang, and S.-L. Zhu, *Phys. Rev. D* **104**, 094003 (2021).
- [52] K. Terasaki, *Prog. Theor. Phys.* **118**, 821 (2007).
- [53] L. Maiani, A. D. Polosa, and V. Riquer, *Phys. Lett. B* **778**, 247 (2018).
- [54] L. Maiani, A. D. Polosa, and V. Riquer, *Phys. Rev. D* **102**, 034017 (2020).

R. Aaij¹², A. S. W. Abdelmotteleb⁵⁰, C. Abellan Beteta⁴⁴, F. Abudinén⁵⁰, T. Ackernley⁵⁴, B. Adeva⁴⁰, M. Adinolfi⁴⁸, H. Afsharnia⁹, C. Agapopoulou¹³, C. A. Aidala⁷⁷, S. Aiola²⁵, Z. Ajaltouni⁹, S. Akar⁵⁹, K. Akiba³², J. Albrecht¹⁵, F. Alessio⁴², M. Alexander⁵³, A. Alfonso Alberro³⁹, Z. Aliouche⁵⁶, P. Alvarez Cartelle⁴⁹, S. Amato², J. L. Amey⁴⁸, Y. Amhis¹¹, L. An⁴², L. Anderlini²², M. Andersson⁴⁴, A. Andreianov³⁸, M. Andreotti²¹, D. Ao⁶, F. Archilli¹⁷, A. Artamonov³⁸, M. Artuso⁶², K. Arzymatov³⁸, E. Aslanides¹⁰, M. Atzeni⁴⁴, B. Audurier¹², S. Bachmann¹⁷, M. Bachmayer⁴³, J. J. Back⁵⁰, A. Bailly-reyre¹³, P. Baladron Rodriguez⁴⁰, V. Balagura¹², W. Baldini²¹, J. Baptista de Souza Leite¹, M. Barbetti^{22,b}, R. J. Barlow⁵⁶, S. Barsuk¹¹, W. Barter⁵⁵, M. Bartolini⁴⁹, F. Baryshnikov³⁸, J. M. Basels¹⁴, G. Bassi^{29,c}, B. Batsukh⁴, A. Battig¹⁵, A. Bay⁴³, A. Beck⁵⁰, M. Becker¹⁵, F. Bedeschi²⁹, I. B. Bediaga¹, A. Beiter⁶², V. Belavin³⁸, S. Belin²⁷, V. Bellee⁴⁴, K. Belous³⁸, I. Belov³⁸, I. Belyaev³⁸, G. Bencivenni²³, E. Ben-Haim¹³, A. Berezhnoy³⁸, R. Bernet⁴⁴, D. Berninghoff¹⁷, H. C. Bernstein⁶², C. Bertella⁵⁶, A. Bertolin²⁸, C. Betancourt⁴⁴, F. Betti⁴², I. Bezshyiko⁴⁴, S. Bhasin⁴⁸, J. Bhom³⁵, L. Bian⁶⁷, M. S. Bieker¹⁵, N. V. Biesuz²¹, S. Bifani⁴⁷, P. Billoir¹³, A. Biolchini³², M. Birch⁵⁵, F. C. R. Bishop⁴⁹, A. Bitadze⁵⁶, A. Bizzeti¹⁵, M. Bjørn⁵⁷, M. P. Blago⁴⁹, T. Blake⁵⁰, F. Blanc⁴³, S. Blusk⁶², D. Bobulska⁵³, J. A. Boelhauve¹⁵, O. Boente Garcia⁴⁰, T. Boettcher⁵⁹, A. Boldyrev³⁸, N. Bondar^{38,42}, S. Borghi⁵⁶, M. Borisyak³⁸, M. Borsato¹⁷, J. T. Borsuk³⁵, S. A. Bouchiba⁴³, T. J. V. Bowcock^{54,42}, A. Boyer⁴², C. Bozzi²¹, M. J. Bradley⁵⁵, S. Braun⁶⁰, A. Brea Rodriguez⁴⁰, J. Brodzicka³⁵, A. Brossa Gonzalo⁵⁰, D. Brundu²⁷, A. Buonaura⁴⁴, L. Buonincontri²⁸, A. T. Burke⁵⁶, C. Burr⁴², A. Bursche⁶⁶, A. Butkevich³⁸, J. S. Butter³², J. Buytaert⁴², W. Byczynski⁴², S. Cadeddu²⁷, H. Cai⁶⁷, R. Calabrese^{21,d}, L. Calefice^{15,13}, S. Cali²³, R. Calladine⁴⁷, M. Calvi^{26,e}, M. Calvo Gomez⁷⁵, P. Camargo Magalhaes⁴⁸, P. Campana²³, A. F. Campoverde Quezada⁶, S. Capelli^{26,e}, L. Capriotti^{20,f}, A. Carbone^{20,f}, G. Carboni³¹

R. Cardinale^{24,g} A. Cardini²⁷ I. Carli⁴ P. Carniti^{26,e} L. Carus,¹⁴ A. Casais Vidal⁴⁰ R. Caspary¹⁷ G. Casse⁵⁴
M. Cattaneo⁴² G. Cavallero⁴² V. Cavallini^{21,d} S. Celani⁴³ J. Cerasoli¹⁰ D. Cervenkov⁵⁷ A. J. Chadwick⁵⁴
M. G. Chapman,⁴⁸ M. Charles¹³ Ph. Charpentier⁴² C. A. Chavez Barajas⁵⁴ M. Chefdeville⁸ C. Chen³
S. Chen⁴ A. Chernov³⁵ V. Chobanova⁴⁰ S. Cholak⁴³ M. Chrzaszcz³⁵ A. Chubykin³⁸ V. Chulikov³⁸
P. Ciambrone²³ M. F. Cicala⁵⁰ X. Cid Vidal⁴⁰ G. Ciezarek⁴² G. Ciullo^{21,d} P. E. L. Clarke⁵² M. Clemencic⁴²
H. V. Cliff⁴⁹ J. Closier⁴² J. L. Cobbledick⁵⁶ V. Coco⁴² J. A. B. Coelho¹¹ J. Cogan¹⁰ E. Cogneras⁹
L. Cojocariu³⁷ P. Collins⁴² T. Colombo⁴² L. Congedo^{19,h} A. Contu²⁷ N. Cooke⁴⁷ G. Coombs⁵³
I. Corredoira⁴⁰ G. Corti⁴² C. M. Costa Sobral⁵⁰ B. Couturier⁴² D. C. Craik⁵⁸ J. Crkovská⁶¹ M. Cruz Torres^{1,i}
R. Currie⁵² C. L. Da Silva⁶¹ S. Dadabaev³⁸ L. Dai⁶⁵ E. Dall’Occo¹⁵ J. Dalseno⁴⁰ C. D’Ambrosio⁴²
A. Danilina³⁸ P. d’Argent⁴² J. E. Davies⁵⁶ A. Davis⁵⁶ O. De Aguiar Francisco⁵⁶ J. de Boer⁴² K. De Bruyn⁷³
S. De Capua⁵⁶ M. De Cian⁴³ U. De Freitas Carneiro Da Graca¹ E. De Lucia²³ J. M. De Miranda¹ L. De Paula²
M. De Serio^{19,h} D. De Simone⁴⁴ P. De Simone²³ F. De Vellis¹⁵ J. A. de Vries⁷⁴ C. T. Dean⁶¹
F. Debernardis^{19,h} D. Decamp⁸ V. Dedu¹⁰ L. Del Buono¹³ B. Delaney⁴⁹ H.-P. Dembinski¹⁵ V. Denysenko⁴⁴
O. Deschamps⁹ F. Dettori^{27,j} B. Dey⁷¹ A. Di Cicco²³ P. Di Nezza²³ S. Didenko³⁸ L. Dieste Maronas⁴⁰
H. Dijkstra⁴² V. Dobishuk⁴⁶ C. Dong³ A. M. Donohoe¹⁸ F. Dordei²⁷ A. C. dos Reis¹ L. Douglas⁵³
A. G. Downes⁸ M. W. Dudek³⁵ L. Dufour⁴² V. Duk⁷² P. Durante⁴² J. M. Durham⁶¹ D. Dutta⁵⁶
A. Dziurda³⁵ A. Dzyuba³⁸ S. Easo⁵¹ U. Egede⁶³ V. Egorychev³⁸ S. Eidelman^{38,a} S. Eisenhardt⁵² S. Ek-In⁴³
L. Eklund⁷⁶ S. Ely⁶² A. Ene³⁷ E. Epple⁶¹ S. Escher¹⁴ J. Eschle⁴⁴ S. Esen⁴⁴ T. Evans⁵⁶ L. N. Falcao¹
Y. Fan⁶ B. Fang⁶⁷ S. Farry⁵⁴ D. Fazzini^{26,e} M. Feo⁴² A. Fernandez Prieto⁴⁰ C. Fernandez-Ramirez^{62,k}
A. D. Fernez⁶⁰ F. Ferrari²⁰ L. Ferreira Lopes⁴³ F. Ferreira Rodrigues² S. Ferreres Sole³² M. Ferrillo⁴⁴
M. Ferro-Luzzi⁴² S. Filippov³⁸ R. A. Fini¹⁹ M. Fiorini^{21,d} M. Firlej³⁴ K. M. Fischer⁵⁷ D. S. Fitzgerald⁷⁷
C. Fitzpatrick⁵⁶ T. Fiutowski³⁴ F. Fleuret¹² M. Fontana¹³ F. Fontanelli^{24,g} R. Forty⁴² D. Foulds-Holt⁴⁹
V. Franco Lima⁵⁴ M. Franco Sevilla⁶⁰ M. Frank⁴² E. Franzoso^{21,d} G. Frau¹⁷ C. Frei⁴² D. A. Friday⁵³
J. Fu⁶ Q. Fuehring¹⁵ E. Gabriel³² G. Galati^{19,h} A. Gallas Torreira⁴⁰ D. Galli^{20,f} S. Gambetta^{52,42} Y. Gan³
M. Gandelman² P. Gandini²⁵ Y. Gao⁵ M. Garau^{27,j} L. M. Garcia Martin⁵⁰ P. Garcia Moreno³⁹
J. García Pardiñas^{26,e} B. Garcia Plana⁴⁰ F. A. Garcia Rosales¹² L. Garrido³⁹ C. Gaspar⁴² R. E. Geertsema³²
D. Gerick¹⁷ L. L. Gerken¹⁵ E. Gersabeck⁵⁶ M. Gersabeck⁵⁶ T. Gershon⁵⁰ D. Gerstel¹⁰ L. Giambastiani²⁸
V. Gibson⁴⁹ H. K. Giemza³⁶ A. L. Gilman⁵⁷ M. Giovannetti^{23,1} A. Gioventù⁴⁰ P. Gironella Gironell³⁹
C. Giugliano^{21,d} K. Gizdov⁵² E. L. Gkougkousis⁴² V. V. Gligorov^{13,42} C. Göbel⁶⁴ E. Golobardes⁷⁵
D. Golubkov³⁸ A. Golutvin^{55,38} A. Gomes^{1,m} S. Gomez Fernandez³⁹ F. Goncalves Abrantes⁵⁷ M. Goncerz³⁵
G. Gong³ I. V. Gorelov³⁸ C. Gotti²⁶ J. P. Grabowski¹⁷ T. Grammatico¹³ L. A. Granado Cardoso⁴²
E. Graugés³⁹ E. Graverini⁴³ G. Graziani⁴ A. T. Grecu³⁷ L. M. Greeven³² N. A. Grieser⁴ L. Grillo⁵⁶
S. Gromov³⁸ B. R. Gruberg Cazon⁵⁷ C. Gu³ M. Guarise^{21,d} M. Guittiere¹¹ P. A. Günther¹⁷ E. Gushchin³⁸
A. Guth¹⁴ Y. Guz³⁸ T. Gys⁴² T. Hadavizadeh⁶³ G. Haefeli⁴³ C. Haen⁴² J. Haimberger⁴² S. C. Haines⁴⁹
T. Halewood-leagas⁵⁴ M. M. Halvorsen⁴² P. M. Hamilton⁶⁰ J. Hammerich⁵⁴ Q. Han⁷ X. Han¹⁷
E. B. Hansen⁵⁶ S. Hansmann-Menzemer¹⁷ L. Hao⁶ N. Harnew⁵⁷ T. Harrison⁵⁴ C. Hasse⁴² M. Hatch⁴²
J. He^{6,n} M. Hecker⁵⁵ K. Heijhoff³² K. Heinicke¹⁵ R. D. L. Henderson^{63,50} A. M. Hennequin⁴² K. Hennessy⁵⁴
L. Henry⁴² J. Heuel¹⁴ A. Hicheur² D. Hill⁴³ M. Hilton⁵⁶ S. E. Hollitt¹⁵ R. Hou⁷ Y. Hou⁸ J. Hu¹⁷
J. Hu⁶⁶ W. Hu⁷ X. Hu³ W. Huang⁶ X. Huang⁶⁷ W. Hulsbergen³² R. J. Hunter⁵⁰ M. Hushchyn³⁸
D. Hutchcroft⁵⁴ D. Hynds³² P. Ibis¹⁵ M. Idzik³⁴ D. Ilin³⁸ P. Ilten⁵⁹ A. Inglessi³⁸ A. Ishteev³⁸
K. Ivshin³⁸ R. Jacobsson⁴² H. Jage¹⁴ S. Jakobsen⁴² E. Jans³² B. K. Jashal⁴¹ A. Jawahery⁶⁰ V. Jevtic¹⁵
X. Jiang^{4,6} M. John⁵⁷ D. Johnson⁵⁸ C. R. Jones⁴⁹ T. P. Jones⁵⁰ B. Jost⁴² N. Jurik⁴² S. Kandybei⁴⁵
Y. Kang³ M. Karacson⁴² D. Karpenkov³⁸ M. Karpov³⁸ J. W. Kautz⁵⁹ F. Keizer⁴² D. M. Keller⁶²
M. Kenzie⁵⁰ T. Ketel³³ B. Khanji¹⁵ A. Kharisova³⁸ S. Kholodenko³⁸ T. Kim¹⁴ V. S. Kirsebom⁴³
O. Kitouni⁵⁸ S. Klaver³³ N. Kleijne^{29,c} K. Klimaszewski³⁶ M. R. Kmiec³⁶ S. Koliiev⁴⁶ A. Kondybayeva³⁸
A. Konoplyannikov³⁸ P. Kopciwicz³⁴ R. Kopecna¹⁷ P. Koppenburg³² M. Korolev³⁸ I. Kostiuik^{32,46} O. Kot⁴⁶
S. Kotriakhova⁴ A. Kozachuk³⁸ P. Kravchenko³⁸ L. Kravchuk³⁸ R. D. Krawczyk⁴² M. Kreps⁵⁰
S. Kretzschmar¹⁴ P. Krokovny³⁸ W. Krupa³⁴ W. Krzemien³⁶ J. Kubat¹⁷ W. Kucewicz^{35,34} M. Kucharczyk³⁵
V. Kudryavtsev³⁸ H. S. Kuindersma³² G. J. Kunde⁶¹ T. Kvaratskheliya³⁸ D. Lacarrere⁴² G. Lafferty⁵⁶ A. Lai²⁷

A. Lampis^{27,j} D. Lancierini⁴⁴ J. J. Lane⁵⁶ R. Lane⁴⁸ G. Lanfranchi²³ C. Langenbruch¹⁴ J. Langer¹⁵
O. Lantwin³⁸ T. Latham⁵⁰ F. Lazzari^{29,o} M. Lazzaroni^{25,p} R. Le Gac¹⁰ S. H. Lee⁷⁷ R. Lefèvre⁹ A. Leflat³⁸
S. Legotin³⁸ P. Lenisa^{21,d} O. Leroy¹⁰ T. Lesiak³⁵ B. Leverington¹⁷ H. Li⁶⁶ P. Li¹⁷ S. Li⁷ Y. Li⁴ Z. Li⁶²
X. Liang⁶² T. Lin⁵⁵ R. Lindner⁴² V. Lisovskyi¹⁵ R. Litvinov^{27,j} G. Liu⁶⁶ H. Liu⁶ Q. Liu⁶ S. Liu^{4,6}
A. Lobo Salvia³⁹ A. Loi²⁷ R. Lollini⁷² J. Lomba Castro⁴⁰ I. Longstaff⁵³ J. H. Lopes² S. López Soliño⁴⁰
G. H. Lovell⁴⁹ Y. Lu^{4,q} C. Lucarelli^{22,b} D. Lucchesi^{28,r} S. Luchuk³⁸ M. Lucio Martinez³²
V. Lukashenko^{32,46} Y. Luo³ A. Lupato⁵⁶ E. Luppi^{21,d} O. Lupton⁵⁰ A. Lusiani^{29,c} X.-R. Lyu⁶ L. Ma⁴
R. Ma⁶ S. Maccolini²⁰ F. Machefert¹¹ F. Maciuc³⁷ V. Macko⁴³ P. Mackowiak¹⁵ S. Maddrell-Mander⁴⁸
L. R. Madhan Mohan⁴⁸ A. Maevskiy³⁸ D. Maisuzenko³⁸ M. W. Majewski³⁴ J. J. Malczewski³⁵ S. Malde⁵⁷
B. Malecki³⁵ A. Malinin³⁸ T. Maltsev³⁸ H. Malygina¹⁷ G. Manca^{27,j} G. Mancinelli¹⁰ D. Manuzzi²⁰
D. Marangotto^{25,p} J. F. Marchand⁸ U. Marconi²⁰ S. Mariani^{22,b} C. Marin Benito⁴² M. Marinangeli⁴³
J. Marks¹⁷ A. M. Marshall⁴⁸ P. J. Marshall⁵⁴ G. Martelli^{72,s} G. Martellotti³⁰ L. Martinazzoli^{42,e}
M. Martinelli^{26,e} D. Martinez Santos⁴⁰ F. Martinez Vidal⁴¹ A. Massafferri¹ M. Materok¹⁴ R. Matev⁴²
A. Mathad⁴⁴ V. Matiunin³⁸ C. Matteuzzi²⁶ K. R. Mattioli⁷⁷ A. Mauri³² E. Maurice¹² J. Mauricio³⁹
M. Mazurek⁴² M. McCann⁵⁵ L. McConnell¹⁸ T. H. McGrath⁵⁶ N. T. McHugh⁵³ A. McNab⁵⁶ R. McNulty¹⁸
J. V. Mead⁵⁴ B. Meadows⁵⁹ G. Meier¹⁵ D. Melnychuk³⁶ S. Meloni^{26,e} M. Merk^{32,74} A. Merli^{25,p}
L. Meyer Garcia² M. Mikhasenko^{69,t} D. A. Milanese⁶⁸ E. Millard⁵⁰ M. Milovanovic⁴² M.-N. Minard^{8,a}
A. Minotti^{26,e} S. E. Mitchell⁵² B. Mitreska⁵⁶ D. S. Mitzel¹⁵ A. Mödden¹⁵ R. A. Mohammed⁵⁷ R. D. Moise⁵⁵
S. Mokhnenko³⁸ T. Mombächer⁴⁰ I. A. Monroy⁶⁸ S. Monteil⁹ M. Morandin²⁸ G. Morello²³
M. J. Morello^{29,c} J. Moron³⁴ A. B. Morris⁶⁹ A. G. Morris⁵⁰ R. Mountain⁶² H. Mu³ F. Muheim⁵²
M. Mulder⁷³ K. Müller⁴⁴ C. H. Murphy⁵⁷ D. Murray⁵⁶ R. Murta⁵⁵ P. Muzzetto^{27,j} P. Naik⁴⁸ T. Nakada⁴³
R. Nandakumar⁵¹ T. Nanut⁴² I. Nasteva² M. Needham⁵² N. Neri^{25,p} S. Neubert⁶⁹ N. Neufeld⁴²
P. Neustroev³⁸ R. Newcombe⁵⁵ E. M. Niel⁴³ S. Nieswand¹⁴ N. Nikitin³⁸ N. S. Nolte⁵⁸ C. Normand^{8,27,j}
C. Nunez⁷⁷ A. Oblakowska-Mucha³⁴ V. Obraztsov³⁸ T. Oeser¹⁴ D. P. O'Hanlon⁴⁸ S. Okamura^{21,d}
R. Oldeman^{27,j} F. Oliva⁵² M. E. Olivares⁶² C. J. G. Onderwater⁷³ R. H. O'Neil⁵² J. M. Otalora Goicochea²
T. Ovsianikova³⁸ P. Owen⁴⁴ A. Oyanguren⁴¹ O. Ozcelik⁵² K. O. Padeken⁶⁹ B. Pagare⁵⁰ P. R. Pais⁴²
T. Pajero⁵⁷ A. Palano¹⁹ M. Palutan²³ Y. Pan⁵⁶ G. Panshin³⁸ A. Papanestis⁵¹ M. Pappagallo^{19,h}
L. L. Pappalardo^{21,d} C. Pappenheimer⁵⁹ W. Parker⁶⁰ C. Parkes⁵⁶ B. Passalacqua^{21,d} G. Passaleva²²
A. Pastore¹⁹ M. Patel⁵⁵ C. Patrignani^{20,f} C. J. Pawley⁷⁴ A. Pearce⁴² A. Pellegrino³² M. Pepe Altarelli⁴²
S. Perazzini²⁰ D. Pereima³⁸ A. Pereiro Castro⁴⁰ P. Perret⁹ M. Petric⁵³ K. Petridis⁴⁸ A. Petrolini^{24,g}
A. Petrov³⁸ S. Petrucci⁵² M. Petruzzolo²⁵ H. Pham⁶² A. Philippov³⁸ R. Piandani⁶ L. Pica^{29,c} M. Piccini⁷²
B. Pietrzyk⁸ G. Pietrzyk¹¹ M. Pili⁵⁷ A. Pilloni^{62,u} D. Pinci³⁰ F. Pisani⁴² M. Pizzichemi^{26,42,e} V. Placinta³⁷
J. Plews⁴⁷ M. Plo Casasus⁴⁰ F. Polci^{13,42} M. Poli Lener²³ M. Poliakov⁶² A. Poluektov¹⁰ N. Polukhina³⁸
I. Polyakov⁶² E. Polycarpo² S. Ponce⁴² D. Popov^{6,42} S. Popov³⁸ S. Poslavskii³⁸ K. Prasanth³⁵
L. Promberger⁴² C. Prouve⁴⁰ V. Pugatch⁴⁶ V. Puill¹¹ G. Punzi^{29,v} H. R. Qi³ W. Qian⁶ N. Qin³
R. Quagliani⁴³ N. V. Raab¹⁸ R. I. Rabadan Trejo⁶ B. Rachwal³⁴ J. H. Rademacker⁴⁸ R. Rajagopalan⁶²
M. Rama²⁹ M. Ramos Pernas⁵⁰ M. S. Rangel² F. Ratnikov³⁸ G. Raven^{33,42} M. Reboud⁸ F. Redi⁴²
F. Reiss⁵⁶ C. Remon Alepuz⁴¹ Z. Ren³ V. Renaudin⁵⁷ P. K. Resmi¹⁰ R. Ribatti^{29,c} A. M. Ricci²⁷
S. Ricciardi⁵¹ K. Rinnert⁵⁴ P. Robbe¹¹ G. Robertson⁵² A. B. Rodrigues⁴³ E. Rodrigues⁵⁴
J. A. Rodriguez Lopez⁶⁸ E. Rodriguez Rodriguez⁴⁰ A. Rollings⁵⁷ P. Roloff⁴² V. Romanovskiy³⁸
M. Romero Lamas⁴⁰ A. Romero Vidal⁴⁰ J. D. Roth^{77,a} M. Rotondo²³ M. S. Rudolph⁶² T. Ruf⁴²
R. A. Ruiz Fernandez⁴⁰ J. Ruiz Vidal⁴¹ A. Ryzhikov³⁸ J. Ryzka³⁴ J. J. Saborido Silva⁴⁰ N. Sagidova³⁸
N. Sahoo⁴⁷ B. Saitta^{27,j} M. Salomoni⁴² C. Sanchez Gras³² R. Santacesaria³⁰ C. Santamarina Rios⁴⁰
M. Santimaria²³ E. Santovetti^{31,1} D. Saranin³⁸ G. Sarpis¹⁴ M. Sarpis⁶⁹ A. Sarti³⁰ C. Satriano^{30,w}
A. Satta³¹ M. Saur¹⁵ D. Savrina³⁸ H. Sazak⁹ L. G. Scantlebury Smead⁵⁷ A. Scarabotto¹³ S. Schael¹⁴
S. Scherl⁵⁴ M. Schiller⁵³ H. Schindler⁴² M. Schmelling¹⁶ B. Schmidt⁴² S. Schmitt¹⁴ O. Schneider⁴³
A. Schopper⁴² M. Schubiger³² S. Schulte⁴³ M. H. Schune¹¹ R. Schwemmer⁴² B. Sciascia^{23,42} A. Sciuccati⁴²
S. Sellam⁴⁰ A. Semennikov³⁸ M. Senghi Soares³³ A. Sergi^{24,g} N. Serra⁴⁴ L. Sestini²⁸ A. Seuthe¹⁵
Y. Shang⁵ D. M. Shangase⁷⁷ M. Shapkin³⁸ I. Shchemerov³⁸ L. Shchutska⁴³ T. Shears⁵⁴ L. Shekhtman³⁸

Z. Shen⁵, S. Sheng^{4,6}, V. Shevchenko³⁸, E. B. Shields^{26,e}, Y. Shimizu¹¹, E. Shmanin³⁸, J. D. Shupperd⁶², B. G. Siddi^{21,d}, R. Silva Coutinho⁴⁴, G. Simi²⁸, S. Simone^{19,h}, N. Skidmore⁵⁶, R. Skuza¹⁷, T. Skwarnicki⁶², M. W. Slater⁴⁷, I. Slazyk^{21,d}, J. C. Smallwood⁵⁷, J. G. Smeaton⁴⁹, E. Smith⁴⁴, M. Smith⁵⁵, A. Snoch³², L. Soares Lavra⁹, M. D. Sokoloff⁵⁹, F. J. P. Soler⁵³, A. Solomin^{38,48}, A. Solovov³⁸, I. Solovyev³⁸, F. L. Souza De Almeida², B. Souza De Paula², B. Spaan^{15,a}, E. Spadaro Norella^{25,p}, E. Spiridenkov³⁸, P. Spradlin⁵³, F. Stagni⁴², M. Stahl⁵⁹, S. Stahl⁴², S. Stanislaus⁵⁷, O. Steinkamp⁴⁴, O. Stenyakin³⁸, H. Stevens¹⁵, S. Stone^{62,a}, D. Strekalina³⁸, F. Suljik⁵⁷, J. Sun²⁷, L. Sun⁶⁷, Y. Sun⁶⁰, P. Svihra⁵⁶, P. N. Swallow⁴⁷, K. Swientek³⁴, A. Szabelski³⁶, A. Szczepaniak^{62,x}, T. Szumlak³⁴, M. Szymanski⁴², S. Taneja⁵⁶, A. R. Tanner⁴⁸, M. D. Tat⁵⁷, A. Terentev³⁸, F. Teubert⁴², E. Thomas⁴², D. J. D. Thompson⁴⁷, K. A. Thomson⁵⁴, H. Tilquin⁵⁵, V. Tisserand⁹, S. T'Jampens⁸, M. Tobin⁴, L. Tomassetti^{21,d}, X. Tong⁵, D. Torres Machado¹, D. Y. Tou³, E. Trifonova³⁸, S. M. Trilov⁴⁸, C. Trippl⁴³, G. Tuci⁶, A. Tully⁴³, N. Tuning^{32,42}, A. Ukleja^{36,42}, D. J. Unverzagt¹⁷, E. Ursov³⁸, A. Usachov³², A. Ustyuzhanin³⁸, U. Uwer¹⁷, A. Vagner³⁸, V. Vagnoni²⁰, A. Valassi⁴², G. Valenti²⁰, N. Valls Canudas⁷⁵, M. van Beuzekom³², M. Van Dijk⁴³, H. Van Hecke⁶¹, E. van Herwijnen³⁸, M. van Veghel⁷³, R. Vazquez Gomez³⁹, P. Vazquez Regueiro⁴⁰, C. Vázquez Sierra⁴², S. Vecchi²¹, J. J. Velthuis⁴⁸, M. Veltri^{22,y}, A. Venkateswaran⁶², M. Veronesi³², M. Vesterinen⁵⁰, D. Vieira⁵⁹, M. Vieites Diaz⁴³, H. Viemann⁷⁰, X. Vilasis-Cardona⁷⁵, E. Vilella Figueras⁵⁴, A. Villa²⁰, P. Vincent¹³, F. C. Volle¹¹, D. vom Bruch¹⁰, A. Vorobyev³⁸, V. Vorobyev³⁸, N. Voropaev³⁸, K. Vos⁷⁴, R. Waldi¹⁷, J. Walsh²⁹, C. Wang¹⁷, J. Wang⁵, J. Wang⁴, J. Wang³, J. Wang⁶⁷, M. Wang⁵, R. Wang⁴⁸, Y. Wang⁷, Z. Wang⁴⁴, Z. Wang³, Z. Wang⁶, J. A. Ward^{50,63}, N. K. Watson⁴⁷, D. Websdale⁵⁵, C. Weisser⁵⁸, B. D. C. Westhenry⁴⁸, D. J. White⁵⁶, M. Whitehead⁴⁸, A. R. Wiederhold⁵⁰, D. Wiedner¹⁵, G. Wilkinson⁵⁷, M. K. Wilkinson⁶², I. Williams⁴⁹, M. Williams⁵⁸, M. R. J. Williams⁵², F. F. Wilson⁵¹, W. Wislicki³⁶, M. Witek³⁵, L. Witola¹⁷, G. Wormser¹¹, S. A. Wotton⁴⁹, H. Wu⁶², K. Wyllie⁴², Z. Xiang⁶, D. Xiao⁷, Y. Xie⁷, A. Xu⁵, J. Xu⁶, L. Xu³, M. Xu⁵⁰, Q. Xu⁶, Z. Xu⁹, Z. Xu⁶, D. Yang³, S. Yang⁶, Y. Yang⁶, Z. Yang⁵, Z. Yang⁶⁰, Y. Yao⁶², L. E. Yeomans⁵⁴, H. Yin⁷, J. Yu⁶⁵, X. Yuan⁶², E. Zaffaroni⁴³, M. Zavertyaev¹⁶, M. Zdybal³⁵, O. Zenaiev⁴², M. Zeng³, D. Zhang⁷, L. Zhang³, S. Zhang⁶⁵, S. Zhang⁵, Y. Zhang⁵, Y. Zhang⁵⁷, A. Zharkova³⁸, A. Zhelezov¹⁷, Y. Zheng⁶, T. Zhou⁶, X. Zhou⁶, Y. Zhou⁶, V. Zhovkovska¹¹, X. Zhu³, X. Zhu⁷, Z. Zhu⁶, V. Zhukov^{14,38}, Q. Zou^{4,6}, S. Zucchelli^{20,f}, D. Zuliani²⁸ and G. Zunica⁵⁶

(LHCb Collaboration)

¹Centro Brasileiro de Pesquisas Físicas (CBPF), Rio de Janeiro, Brazil²Universidade Federal do Rio de Janeiro (UFRJ), Rio de Janeiro, Brazil³Center for High Energy Physics, Tsinghua University, Beijing, China⁴Institute Of High Energy Physics (IHEP), Beijing, China⁵School of Physics State Key Laboratory of Nuclear Physics and Technology, Peking University, Beijing, China⁶University of Chinese Academy of Sciences, Beijing, China⁷Institute of Particle Physics, Central China Normal University, Wuhan, Hubei, China⁸Université Savoie Mont Blanc, CNRS, IN2P3-LAPP, Annecy, France⁹Université Clermont Auvergne, CNRS/IN2P3, LPC, Clermont-Ferrand, France¹⁰Aix Marseille Univ, CNRS/IN2P3, CPPM, Marseille, France¹¹Université Paris-Saclay, CNRS/IN2P3, IJCLab, Orsay, France¹²Laboratoire Leprince-Ringuet, CNRS/IN2P3, Ecole Polytechnique, Institut Polytechnique de Paris, Palaiseau, France¹³LPNHE, Sorbonne Université, Paris Diderot Sorbonne Paris Cité, CNRS/IN2P3, Paris, France¹⁴I. Physikalisches Institut, RWTH Aachen University, Aachen, Germany¹⁵Fakultät Physik, Technische Universität Dortmund, Dortmund, Germany¹⁶Max-Planck-Institut für Kernphysik (MPIK), Heidelberg, Germany¹⁷Physikalisches Institut, Ruprecht-Karls-Universität Heidelberg, Heidelberg, Germany¹⁸School of Physics, University College Dublin, Dublin, Ireland¹⁹INFN Sezione di Bari, Bari, Italy²⁰INFN Sezione di Bologna, Bologna, Italy²¹INFN Sezione di Ferrara, Ferrara, Italy

- ²²*INFN Sezione di Firenze, Firenze, Italy*
- ²³*INFN Laboratori Nazionali di Frascati, Frascati, Italy*
- ²⁴*INFN Sezione di Genova, Genova, Italy*
- ²⁵*INFN Sezione di Milano, Milano, Italy*
- ²⁶*INFN Sezione di Milano-Bicocca, Milano, Italy*
- ²⁷*INFN Sezione di Cagliari, Monserrato, Italy*
- ²⁸*Università degli Studi di Padova, Università e INFN, Padova, Padova, Italy*
- ²⁹*INFN Sezione di Pisa, Pisa, Italy*
- ³⁰*INFN Sezione di Roma La Sapienza, Roma, Italy*
- ³¹*INFN Sezione di Roma Tor Vergata, Roma, Italy*
- ³²*Nikhef National Institute for Subatomic Physics, Amsterdam, Netherlands*
- ³³*Nikhef National Institute for Subatomic Physics and VU University Amsterdam, Amsterdam, Netherlands*
- ³⁴*AGH—University of Science and Technology,
Faculty of Physics and Applied Computer Science, Kraków, Poland*
- ³⁵*Henryk Niewodniczanski Institute of Nuclear Physics Polish Academy of Sciences, Kraków, Poland*
- ³⁶*National Center for Nuclear Research (NCBJ), Warsaw, Poland*
- ³⁷*Horia Hulubei National Institute of Physics and Nuclear Engineering, Bucharest-Magurele, Romania*
- ³⁸*Affiliated with an institute covered by a cooperation agreement with CERN*
- ³⁹*ICCUB, Universitat de Barcelona, Barcelona, Spain*
- ⁴⁰*Instituto Galego de Física de Altas Enerxías (IGFAE), Universidade de Santiago de Compostela,
Santiago de Compostela, Spain*
- ⁴¹*Instituto de Física Corpuscular, Centro Mixto Universidad de Valencia—CSIC, Valencia, Spain*
- ⁴²*European Organization for Nuclear Research (CERN), Geneva, Switzerland*
- ⁴³*Institute of Physics, Ecole Polytechnique Fédérale de Lausanne (EPFL), Lausanne, Switzerland*
- ⁴⁴*Physik-Institut, Universität Zürich, Zürich, Switzerland*
- ⁴⁵*NSC Kharkiv Institute of Physics and Technology (NSC KIPT), Kharkiv, Ukraine*
- ⁴⁶*Institute for Nuclear Research of the National Academy of Sciences (KINR), Kyiv, Ukraine*
- ⁴⁷*University of Birmingham, Birmingham, United Kingdom*
- ⁴⁸*H.H. Wills Physics Laboratory, University of Bristol, Bristol, United Kingdom*
- ⁴⁹*Cavendish Laboratory, University of Cambridge, Cambridge, United Kingdom*
- ⁵⁰*Department of Physics, University of Warwick, Coventry, United Kingdom*
- ⁵¹*STFC Rutherford Appleton Laboratory, Didcot, United Kingdom*
- ⁵²*School of Physics and Astronomy, University of Edinburgh, Edinburgh, United Kingdom*
- ⁵³*School of Physics and Astronomy, University of Glasgow, Glasgow, United Kingdom*
- ⁵⁴*Oliver Lodge Laboratory, University of Liverpool, Liverpool, United Kingdom*
- ⁵⁵*Imperial College London, London, United Kingdom*
- ⁵⁶*Department of Physics and Astronomy, University of Manchester, Manchester, United Kingdom*
- ⁵⁷*Department of Physics, University of Oxford, Oxford, United Kingdom*
- ⁵⁸*Massachusetts Institute of Technology, Cambridge, Massachusetts, USA*
- ⁵⁹*University of Cincinnati, Cincinnati, Ohio, USA*
- ⁶⁰*University of Maryland, College Park, Maryland, USA*
- ⁶¹*Los Alamos National Laboratory (LANL), Los Alamos, New Mexico, USA*
- ⁶²*Syracuse University, Syracuse, New York, USA*
- ⁶³*School of Physics and Astronomy, Monash University, Melbourne, Australia
(associated with Department of Physics, University of Warwick, Coventry, United Kingdom)*
- ⁶⁴*Pontifícia Universidade Católica do Rio de Janeiro (PUC-Rio), Rio de Janeiro, Brazil
(associated with Universidade Federal do Rio de Janeiro (UFRJ), Rio de Janeiro, Brazil)*
- ⁶⁵*Physics and Micro Electronic College, Hunan University, Changsha City, China
(associated with Institute of Particle Physics, Central China Normal University, Wuhan, Hubei, China)*
- ⁶⁶*Guangdong Provincial Key Laboratory of Nuclear Science, Guangdong-Hong Kong Joint Laboratory of
Quantum Matter, Institute of Quantum Matter, South China Normal University, Guangzhou, China
(associated with Center for High Energy Physics, Tsinghua University, Beijing, China)*
- ⁶⁷*School of Physics and Technology, Wuhan University, Wuhan, China
(associated with Center for High Energy Physics, Tsinghua University, Beijing, China)*
- ⁶⁸*Departamento de Física, Universidad Nacional de Colombia, Bogota, Colombia
(associated with LPNHE, Sorbonne Université, Paris Diderot Sorbonne Paris Cité,
CNRS/IN2P3, Paris, France)*
- ⁶⁹*Universität Bonn—Helmholtz-Institut für Strahlen und Kernphysik, Bonn, Germany
(associated with Physikalisches Institut, Ruprecht-Karls-Universität Heidelberg, Heidelberg, Germany)*

⁷⁰*Institut für Physik, Universität Rostock, Rostock, Germany*
(associated with Physikalisches Institut, Ruprecht-Karls-Universität Heidelberg,
Heidelberg, Germany)

⁷¹*Eotvos Lorand University, Budapest, Hungary*
(associated with European Organization for Nuclear Research (CERN), Geneva, Switzerland)

⁷²*INFN Sezione di Perugia, Perugia, Italy*
(associated with INFN Sezione di Ferrara, Ferrara, Italy)

⁷³*Van Swinderen Institute, University of Groningen, Groningen, Netherlands*
(associated with Nikhef National Institute for Subatomic Physics, Amsterdam, Netherlands)

⁷⁴*Universiteit Maastricht, Maastricht, Netherlands*
(associated with Nikhef National Institute for Subatomic Physics, Amsterdam, Netherlands)

⁷⁵*DS4DS, La Salle, Universitat Ramon Llull, Barcelona, Spain*
(associated with ICCUB, Universitat de Barcelona, Barcelona, Spain)

⁷⁶*Department of Physics and Astronomy, Uppsala University, Uppsala, Sweden*
(associated with School of Physics and Astronomy, University of Glasgow, Glasgow, United Kingdom)

⁷⁷*University of Michigan, Ann Arbor, Michigan, USA*
(associated with Syracuse University, Syracuse, New York, USA)

^aDeceased.

^bAlso at Università di Firenze, Firenze, Italy.

^cAlso at Scuola Normale Superiore, Pisa, Italy.

^dAlso at Università di Ferrara, Ferrara, Italy.

^eAlso at Università di Milano Bicocca, Milano, Italy.

^fAlso at Università di Bologna, Bologna, Italy.

^gAlso at Università di Genova, Genova, Italy.

^hAlso at Università di Bari, Bari, Italy.

ⁱAlso at Universidad Nacional Autónoma de Honduras, Tegucigalpa, Honduras.

^jAlso at Università di Cagliari, Cagliari, Italy.

^kAlso at Departamento de Física Interdisciplinar, Universidad Nacional de Educación a Distancia (UNED), Madrid, Spain.

^lAlso at Università di Roma Tor Vergata, Roma, Italy.

^mAlso at Universidade Federal do Triângulo Mineiro (UFTM), Uberaba-MG, Brazil.

ⁿAlso at Hangzhou Institute for Advanced Study, UCAS, Hangzhou, China.

^oAlso at Università di Siena, Siena, Italy.

^pAlso at Università degli Studi di Milano, Milano, Italy.

^qAlso at Central South U., Changsha, China.

^rAlso at Università di Padova, Padova, Italy.

^sAlso at Università di Perugia, Perugia, Italy.

^tAlso at Excellence Cluster ORIGINS, Munich, Germany.

^uAlso at Dipartimento MIFT, Università degli Studi di Messina and INFN Sezione di Catania, Italy, Messina and Catania, Italy.

^vAlso at Università di Pisa, Pisa, Italy.

^wAlso at Università della Basilicata, Potenza, Italy.

^xAlso at Department of Physics, Indiana University, Bloomington, Indiana, USA.

^yAlso at Università di Urbino, Urbino, Italy.